

Algorithm for detecting sea sky-line based on watershed segmentation

Xun Zhang^{a,b}, Xuejie Guan^b, Jing Luo^b, Yan Zheng^{*a}

^aCollege of Intelligent Systems Science and Engineering, Harbin Engineering University, Harbin 150001, Heilongjiang, China; ^bQingdao Innovation and Development Center, Harbin Engineering University, Qingdao 266000, Shandong, China

ABSTRACT

Sea sky-line detection is crucial for unmanned vessel attitude estimation and maritime surveillance target detection to reduce computational complexity. Many existing seas sky-line detection algorithms mainly extract sea sky-lines through edge detection, but these methods are less robust and susceptible to water surface ripple interference. In this paper, we propose a sea sky-line detection algorithm based on watershed segmentation, which uses the local binarization method to locate the sea sky-line region, segments the connectivity region by watershed algorithm, selects the straight-line pixel points, and accurately calculates the slope and intercept of the sea sky-line using the LSD and RANSAC algorithms. The experimental results show that the algorithm can accurately detect horizontal lines with less error and outperforms the other five advanced algorithms.

Keywords: Sea sky-line detection, watershed segmentation, LSD line detection, RANSAC line fitting, marine environment

1. INTRODUCTION

Sea sky-line has different definitions in different scenarios, but the goal of sea sky-line detection is to accurately segment the sea from the sky¹. In images of the sea or other waters, the boundary between the sea and the sky is an important reference line that can help to identify target objects as well as analyze the environment. Through sea sky-line detection, we can distinguish the water part of the image from the sky part, which provides the basis for subsequent target detection and analysis. Examples include sea target detection², ship attitude fusio³, and image alignment⁴. The currently existing algorithms for sea sky-line detection are categorized into three main groups: edge-based detection⁵, region growth-based⁶, and machine-learning or deep-learning based segmentation⁷. Some algorithms increase speed by quickly locating the ROI of the sea sky-line but may cause localization errors in complex conditions like dense clouds or tilted lines. Edge detection faces challenges with variable edge values under different weather conditions, requiring threshold adjustments that may introduce false edges. Additionally, color feature-based filtering and VGG-16 classifiers, though effective in experiments, may be inefficient and computationally intensive in real-world applications. The region growing algorithm, suitable for high-resolution images, suffers from high time complexity and dependency on seed points, making it unsuitable for color gradient scenes. These issues highlight the need for further optimization of sea sky-line detection algorithms. This paper proposes a hybrid algorithm combining grayscale analysis, texture, gradient watershed, and horizontal line estimation to enhance detection in complex sea conditions. The process involves segmenting the image based on grayscale histogram characteristics, setting segmentation thresholds using histogram variance, distinguishing sky regions using morphological operations, and segmenting using region growing and watershed algorithms. The optimized LSD and RANSAC methods improve Line detection accuracy and speed.

2. METHOD

This section begins with an analysis of the maritime image characteristics, followed by a detailed description of the three main steps of the algorithm proposed in this paper.

2.1 Sea sky-line area detection

Uneven sunlight affects global threshold segmentation of ocean and sky regions due to varying light spots on the sea surface. Before calculating the maximum interclass variance between sea and sky, the grayscale image is divided into N

*yanzheng3@hrbeu.edu.cn; phone 13573836456

(N=12) equal subregions horizontally, as shown in Figure 1.



Figure 1. Schematic diagram of horizontally divided subregions.

A connected-domain filtering algorithm (MPA) using binary morphological operations is proposed to address noise from sea surface ripples and ship wake. The sky and sea are binarized into white and black using adaptive thresholding. Sea surface white noise is removed with a 7×7 square structural element open operation, resulting in Img_{open}^1 . Sky black noise is filtered with a close operation using the same element, producing Img_{close}^2 . Foreground (Img_{front}^3) and background (Img_{back}^3) images are generated using 3×3 cross structural elements for expansion and erosion. By calculating the difference between these images and analyzing connectivity components, unknown regions are marked as -1, identifying the sea-sky line region $img_{unknown}$ for detection (Figure 2).

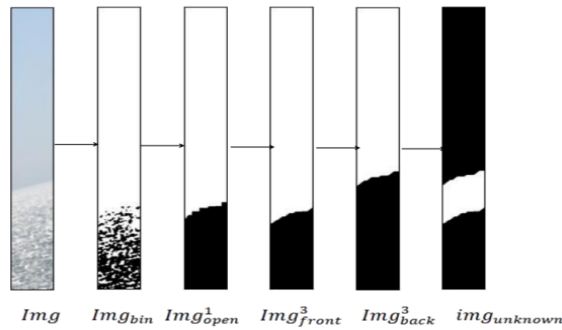


Figure 2. Schematic diagram of morphological processing.

2.2 Watershed detection sea sky-line alternative points

In this paper, median filter preprocessing is used to smooth the sharp part of the sea surface image and retain the image edge details. The $img_{unknown}$ image is used as the mask of watershed segmentation, and only the segmentation lines of the sky and sea surface are calculated, ignoring the internal details of the image. We no longer use the gray scale value, but the gradient value in the neighborhood of the pixel (this paper adopts the four-neighborhood) as the condition of the region growth order, and the formula of the gradient value is as follows:

$$\text{Diff}_{[(x,y),(i,j)]} = \text{Max} \left(\text{src}_{r(x,y)} - \text{src}_{r(i,j)}, \text{src}_{g(x,y)} - \text{src}_{g(i,j)}, \text{src}_{b(x,y)} - \text{src}_{b(i,j)} \right) \quad (1)$$

$$\text{Grads}_{(x,y)} = \text{Min} \left(\text{Diff}_{[(x,y),(x+1,y)]}, \text{Diff}_{[(x,y),(x-1,y)]}, \text{Diff}_{[(x,y),(x,y+1)]}, \text{Diff}_{[(x,y),(x,y-1)]} \right) \quad (2)$$

where $\text{src}_{r(x,y)}$ denotes the grayscale value of the red channel with (x,y) coordinates of the original image, $\text{src}_{g(x,y)}$ denotes the grayscale value of the green channel with (x,y) coordinates of the original image, and $\text{src}_{b(x,y)}$ denotes the grayscale value of the blue channel with (x,y) coordinates of the original image.

Improved watershed segmentation algorithm flow:

- (1) A three-channel color map src and mask are input.
- (2) Label sky in mask as 1, sea as 2, and unknown areas as 0.

- (3) Gradient values for pixels labeled 0 and those >0 in their four neighboring domains are calculated. These values and their corresponding coordinates are then saved to the end of the appropriate priority queue level.
- (4) Step 3 is repeated until all mask pixels are traversed.
- (5) The pixel with the smallest gradient value is popped from the queue. Its four neighbors are checked to determine if more than one pixel is labeled >0 . If so, the pixel is labeled as -1; otherwise, it is assigned the label of a neighboring pixel >0 . Any neighboring pixels labeled 0 are then pushed to the queue.
- (6) Step 5 is repeated until the queue is emptied.
- (7) The mask is returned, with pixels labeled -1 being marked as the watershed. The original image is visualized with watershed pixels shown in blue, as illustrated in Figure 3.



Figure 3. Map of watershed segmentation results.

2.3 Sea sky-line fitting

In order to further eliminate the influence of non-marine antenna pixels on straight line fitting, the filtered pixel points are extracted by LSD straight line detection, line filtering, and extraction. Finally, in this paper, the parameters are fitted by RANSAC algorithm.

Algorithm 1 Sea sky-line Fitting

Input: binary mask map of watershed results $mask_{bin}$.

1: The LSD algorithm is used to detect the line segments in the sub $mask_{bin}$ to get $Line_m$.

2: Calculate the angle of each line segment, $Angle_1, Angle_2, Angle_3, \dots, Angle_m$.

3: for $i=1,2, \dots, m$:

if ($abs(Angle_i) < 40$):

for pixel in $Line_i$:

if pixel in $mask_{bin} == 255$:

$q.push_back(pixel)$

4: for i in range(epoch):

Two pixels are randomly selected from q , and $w_i, b_i, Angle_i$ are calculated, and $abs(Angle) < 40$.

$total_{in} = 0$

for pixel in q :

$y_e = w_i * pixel_x + b_i$

if $abs(y_e - pixel_y) < epsilon$: $total_{in} + +$

Record the parameters w_i and b_i of the maximum $total_{in}$ as w_{final} and b_{final} .

Output: fitted sea sky-line parameters w_{final}, b_{final}

According to the above algorithm, the results are shown in Figures 4(a)-4(e).

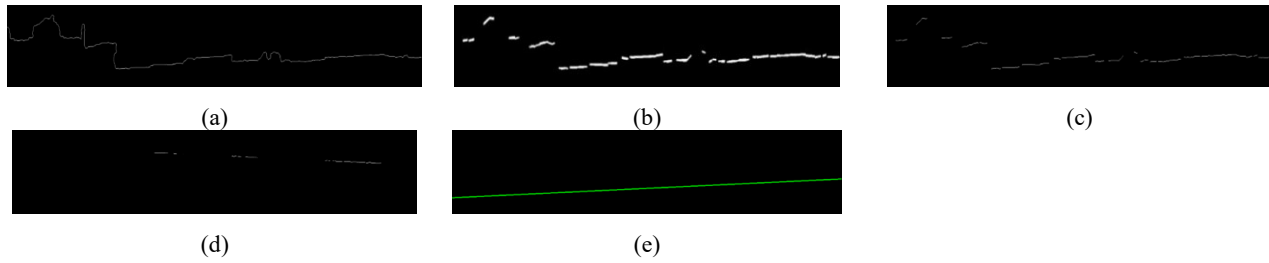


Figure 4. Schematic diagram of the sea sky-line fit.

3. EXPERIMENTAL RESULT

To evaluate the performance of the algorithm in this paper, it is compared with five state-of-the-art methods: ngdsac_horizo⁸: deep learning method, fitting noisy data, including image segmentation, cascade filtering, and line-of-sight extraction. gbhld algorithm⁹: graph-based detection of line-of-sight covering image segmentation, cascade filtering, and sea-sky antennae extraction. wt algorit¹⁰: localization of the sea-sky region by weighting the distribution of texture sea-antenna region using canny and hough straight line detection. MSCM algorithm¹¹: uses multi-scale cross-modal linear features. H-CI algorithm¹²: combines color intensity vectors with covariance matrix. To fully validate the performance, three datasets are used: the Singapore Maritime SMD, Buoy, and MU-SID¹³.

This experiment uses an R7-5800h CPU and Nvidia GTX3060 GPU. H-CI, MSCM, and WT run on Matlab2021a, while GBHLD, ngdsac_horizon, and the proposed method run in a vscode+Python 3.8 environment. Notably, ngdsac_horizon is a deep learning method, training three models on three datasets with a 7:3 train:test split. The loss curve stabilizes at epoch 40, as shown in Figure 5. The final ngdsac_horizon result averages the error across the three datasets for each model.

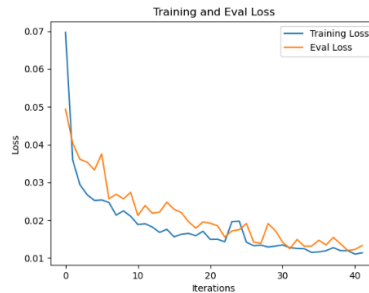


Figure 5. Ngdsac_horizon loss curve.

3.1 Evaluation criteria

This paper conducts comparative experiments with the SMD dataset and a proposed sea sky-line description method to assess detection performance. The angle α of the sea sky-line relative to the horizontal X-axis and the Y-axis coordinate Y of the line's midpoint are used, as shown in Figure 6. α^{error} and Y^{error} are calculated by comparing predicted α and Y values with labeled dataset values, with results expressed in mean and variance. The calculation formula is provided below:

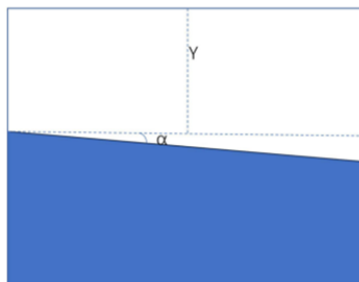


Figure 6. Schematic diagram of evaluation indicators for marine antennas.

$$\alpha_{mean}^{error} = \frac{1}{n} \sum_{i=1}^n |\alpha_i^{test} - \alpha_i^{gt}| \quad Y_{mean}^{error} = \frac{1}{n} \sum_{i=1}^n |Y_i^{test} - Y_i^{gt}| \quad (3)$$

where n denotes the total number of frames in the dataset, this paper defines the evaluation metrics for the sea sky-line detection algorithm: α_i^{test} is the predicted sea sky-line angle to the X-axis in the i th frame of the image, and α_i^{gt} is the true angle, whose accuracy is measured by the α_{mean}^{error} (the average error between the predicted angle and the true angle). Similarly, Y_i^{test} is the coordinates of the predicted midpoint of the sea sky-line in the Y-axis, and Y_i^{gt} is the true coordinates, whose accuracy is measured by Y_{mean}^{error} (the average error between the predicted and true Y-axis coordinates).

In this paper, the same evaluation criteria as those used in the literature are used, namely: vertical position error, standard deviation of vertical position error, angular error and standard deviation of angle error. Tables 1-3 correspond to the data:

Table 1. Evaluation results of the MU-SID dataset.

Method	Evaluation indicators			
	α_{mean}^{error}	α_{std}^{error}	Y_{mean}^{error}	Y_{std}^{error}
MSCM	2.276	6.499	295.633	783.468
H-CI	2.145	5.817	209.483	652.076
GBHLD	3.198	6.731	199.498	276.713
WT	3.040	6.792	133.478	206.907
Ngdsac_horizon	1.342	3.239	40.253	126.079
Proposed	0.207	0.630	26.060	117.989

Table 2. Evaluation results of the BOUY dataset.

Method	Evaluation indicators			
	α_{mean}^{error}	α_{std}^{error}	Y_{mean}^{error}	Y_{std}^{error}
MSCM	0.563	0.783	4.240	15.012
H-CI	3.863	5.188	139.267	116.251
GBHLD	2.946	5.133	52.861	74.115
WT	0.385	0.677	3.094	17.691
Ngdsac_horizon	0.521	0.534	2.344	1.981
Proposed	0.294	0.393	1.573	1.269

Table 3. Evaluation results of the SMD dataset.

Method	Evaluation indicators			
	α_{mean}^{error}	α_{std}^{error}	Y_{mean}^{error}	Y_{std}^{error}
MSCM	1.510	2.253	218.240	214.682
H-CI	1.338	2.024	83.338	78.188
GBHLD	1.104	3.223	27.552	79.399
WT	0.411	0.723	15.798	50.078
Ngdsac_horizon	0.328	0.787	10.259	26.881
Proposed	0.182	0.169	2.875	6.543

3.2 Analysis of results

From the above three representative datasets, it can be seen that the method proposed in this paper has the smallest average localization error (Y_{mean}^{error}) or average angular error (α_{mean}^{error}) and variance value, which is enough to prove the effectiveness of this algorithm. In addition, the proposed method in this paper is able to control the angular error in all three datasets below 0.3, which is significantly better than other algorithms.

4. CONCLUSION

In this paper, a new visible light sea antenna detection algorithm is proposed, which is accurate and stable. Through the comparison experiments with the most advanced five types of algorithms in the three types of data set that are currently public, the algorithm proposed in this paper achieves the best accuracy and robustness, which proves that the sea antenna detection algorithm in the visible light image has good accuracy and robustness, and can overcome the adverse effects of interference such as image blurring, ship wake, large sea antenna inclination angle, and ship occlusion.

ACKNOWLEDGEMENT

This work is supported by NSFC Grant No. 62101156.

REFERENCE

- [1] Liang, D., Zhang, W., Huang, Q., et al., "Robust sea-sky-line detection for complex sea background," 2015 IEEE International Conference on Progress in Informatics and Computing (PIC), 317-321 (2015).
- [2] Dong, L., Ma, D. and Ma, D., "Fast infrared horizon detection algorithm based on gradient directional filtration," J. Opt. Soc. Am. Opt. Image Sci. Vis. 37(11), 1795-1805 (2020).
- [3] Jiang, C., Jiang, H., Zhang, C. and Wang, J., "A new method of sea-sky-line detection," 2010 Third International Symposium on Intelligent Information Technology and Security Informatics, 740-743, (2010).
- [4] Liu, H., "Image processing technology based on computer vision algorithm," Computer & Digital Engineering, (2019).
- [5] Gershikov, E., Libe, T. and Kosolapov, S., "Horizon line detection in marine images: Which method to choose?" Environmental Science 6, 79-88 (2013).
- [6] Zafarifar, B. and Weda, H., "Horizon detection based on sky-color and edge features," Conference on Visual Communications and Image Processing, (2008).
- [7] Girshick, R. B., Donahue, J., Darrell, T., et al., "Rich feature hierarchies for accurate object detection and semantic segmentation," 2014 IEEE Conference on Computer Vision and Pattern Recognition, 580-587 (2013).
- [8] Brachmann, E. and Rother, C., "Neural-Guided RANSAC: Learning where to sample model hypotheses," 2019 IEEE/CVF International Conference on Computer Vision (ICCV), (2019).
- [9] Xu, Y., et al., "Graph-based horizon line detection for UAV navigation," IEEE Journal of Selected Topics in Applied Earth Observations and Remote Sensing, (2021).
- [10] Ganbold, U., Sato, J. and Akashi, T., "Coarse-to-Fine evolutionary method for fast horizon detection in maritime images," IEICE Trans. Inf. & Syst., 2226-2236 (2021)
- [11] Prasad, D. K., Rajan, D., Prasath, C. K., Rachmawati, L., Rajabaly, E. and Quek, C., "MSCM-LiFe: Multi-scale cross modal linear feature for horizon detection in maritime images," 2016 IEEE Region 10 Conference (TENCON), (2017).
- [12] Fefilatye, S., Goldgof, D., Shreve, M. and Lembke, C., "Detection and tracking of ships in open sea with rapidly moving buoy-mounted camera system," Ocean Engineering 54, 1-12 (2012).
- [13] Hashmani, M. A. and Umair, M., "A novel visual-range sea image dataset for sea horizon line detection in changing maritime scenes," JMSE 10, 19 (2022).